NASA CR-54463
BRLD NO. 2978

Final Report

DESIGN, FABRICATION AND TEST OF A FLUID INTERACTION SERVOVALVE

Prepared Under
the Direction of: M. H. Cardon

M. H. Cardon, Project Engineer
Machine and Propulsion Controls Department
Energy Conversion and Dynamic Controls Laboratory

Approved by: L. B. Taplin

L. B. Taplin, Manager
Energy Conversion and Dynamic Controls Laboratory
Technical Director, Fluid State Programs

Prepared for

NATIONAL AERONAUTICS AND SPACE ADMINSTRATION

May 17, 1965

$2.00

CONTRACT NAS 3-5212

Technical Management
NASA Lewis Research Center
Cleveland, Ohio
Advanced Development and Evaluation Division
Vernon D. Gebben

By

The Bendix Corporation
Research Laboratories Division
Southfield, Michigan

TABLE OF CONTENTS

LIST OF ILLUSTRATIONS

LIST OF TABLES

ABSTRACT

31178

A laboratory model of a pneumatic-input servovalve that operates without the use of moving mechanical parts was built and tested. Interactions of fluid streams have been used instead of moving parts. This servovalve has the output characteristics of a four-way open-centered valve. The model was designed to operate with supply pressure of 5.16×10^5 N/m^2 g (75 psig) air and with standard atmosphere (14.7 psia) exhaust. Tests demonstrated a 60 percent pressure recovery and a 44 percent flow recovery. The report presents design details, test results, and suggestions for improving performance.

Author

SECTION 1

INTRODUCTION

In comparison with typical designs of conventional servovalves, designs based on the fluid interaction principle offer important advantages in reliability and maintenance. There are no close-fitting, rubbing parts which may bind or operate erractically, and it is possible to avoid high alternating stresses that commonly lead to fatigue failure. Thus the fluid interaction design is particularly attractive for implementing servovalves which must operate in severe environments of nuclear radiation, extreme temperature, intense shock, and vibration.

The feasibility of implementing a practical fluid interaction servovalve was investigated by designing, fabricating, and testing a laboratory model. The results of this effort are summarized in Section 2. Section 3 reviews the fluid interaction principle and describes the design of the model. Section 4 outlines test procedures and discusses test results. Section 5 gives conclusions and recommendations. Earlier work on this program was presented in NASA quarterly reports CR-54210 and CR-54283, both of which are entitled "Design, Fabrication and Test of a Fluid Interaction Servovalve." This program was carried out under NASA Contract Number NAS 3-5212.

SECTION 2

SUMMARY

A laboratory-type pneumatic servovalve using elements that operate on the interaction of fluid (air) streams was designed, built, and tested. The servovalve has no moving mechanical parts. The pneumatic input signal is below the servovalve supply pressure and less than the pressure differential the servovalve generates. The output characteristics are similar to those of a four-way open-centered-servovalve.

The servovalve is made up of a power stage and a pilot stage. The fluid interaction elements are vortex devices with the exception of Venjet amplifiers used in the pilot stage. The power stage of the servovalve uses two vortex pressure amplifiers. The receivers of these amplifiers form the output ports of the servovalve. Each vortex pressure amplifier of the power stage is controlled by a Venjet amplifier in the pilot stage. The Venjet amplifier consists of a nozzle and receiver enclosed in a chamber. The receiver output pressure and flow vary as function of chamber pressure. The chamber pressure of the Venjet is at a much lower pressure than output receiver pressure and is controlled by a vortex valve that restricts the flow out of the chamber. The input signals to these vortex valves are the input signal to the servovalve. The Venjet in conjunction with the vortex valves allows a low pressure input signal to control a higher level of output pressure.

Table 2-1 summarizes significant performance characteristics and compares them with design specifications. Characteristics such as threshold, symmetry, and hysteresis were also evaluated and were as specified and comparable to a conventional servovalve. The servovalve characteristic pressure-flow curves were somewhat better than a straight line. The input power, flow recovery, and the quiescent supply flow did not meet specified values, but these characteristics can be improved to more nearly meet the specified values by merely optimizing the sizes of the pilot and power stages. The characteristics requiring more refinement are linearity and output noise.

The performance characteristics achieved with the laboratory model of fluid interaction servovalve demonstrates the feasibility of this type servovalve.

Table 2-1 - Summary of Significant Performance Characteristic

ITEM	SPECIFIED	MEASURED
1. Supply Pressure	5.16×10^5 N/m^2 g air (75 psig)	5.16×10^5 N/m^2 g air (75 psig)
2. Pressure Recovery	3.1×10^5 N/m^2 g min (45 psi)	3.1×10^5 N/m^2 (45 psi)
3. Rated No-Load Output Flow	0.0113 Kg/sec (0.025 pps)	0.0131 Kg/sec (0.029 pps)
4. Flow Recovery	0.55 min	0.44
5. Quiescent Supply Flow	0.0204 Kg/sec max (0.045 pps)	0.030 Kg/sec (0.067 pps)
6. Input Signal Pressure	2.75×10^5 N/m^2 g max (40 psig)	1.72×10^5 N/m^2 g (25 psig)
7. Input Signal Bias Pressure	1.38×10^5 N/m^2 g max (20 psig)	1.17×10^5 N/m^2 g (17 psig)
8. Input Signal Power	30 watts max	55 watts
9. Differential Input Signal Power Change for Output Pressure Change From -0.69×10^5 N/m^2 to $+0.69 \times 10^5$ N/m^2 (-10 to +10 psi)	5 watts max	5 watts
10. Linearity $\frac{\text{Gain Max}}{\text{Gain Min}}$	3	15
11. Output Stability	0.034×10^5 N/m^2 max (0.5 psi)	0.27×10^5 N/m^2 (4 psi)
12. Transient Response	0.25 sec	0.10 sec

P-3034

SECTION 3

DESCRIPTION OF SERVOVALVE

The fluid-interaction servovalve is a pneumatic input, four-way open centered valve consisting of a pilot stage and a power stage. A schematic, assembly drawing, and photograph of the servovalve are shown in Figures 3-1, 3-2, and 3-3, respectively.

The pilot stage amplifies the input signal and raises the pressure level to a level compatible with the power stage. The power stage has pressure-flow characteristics similar to that of the conventional four-way bridge, spool type valve. The fluid interaction devices used to

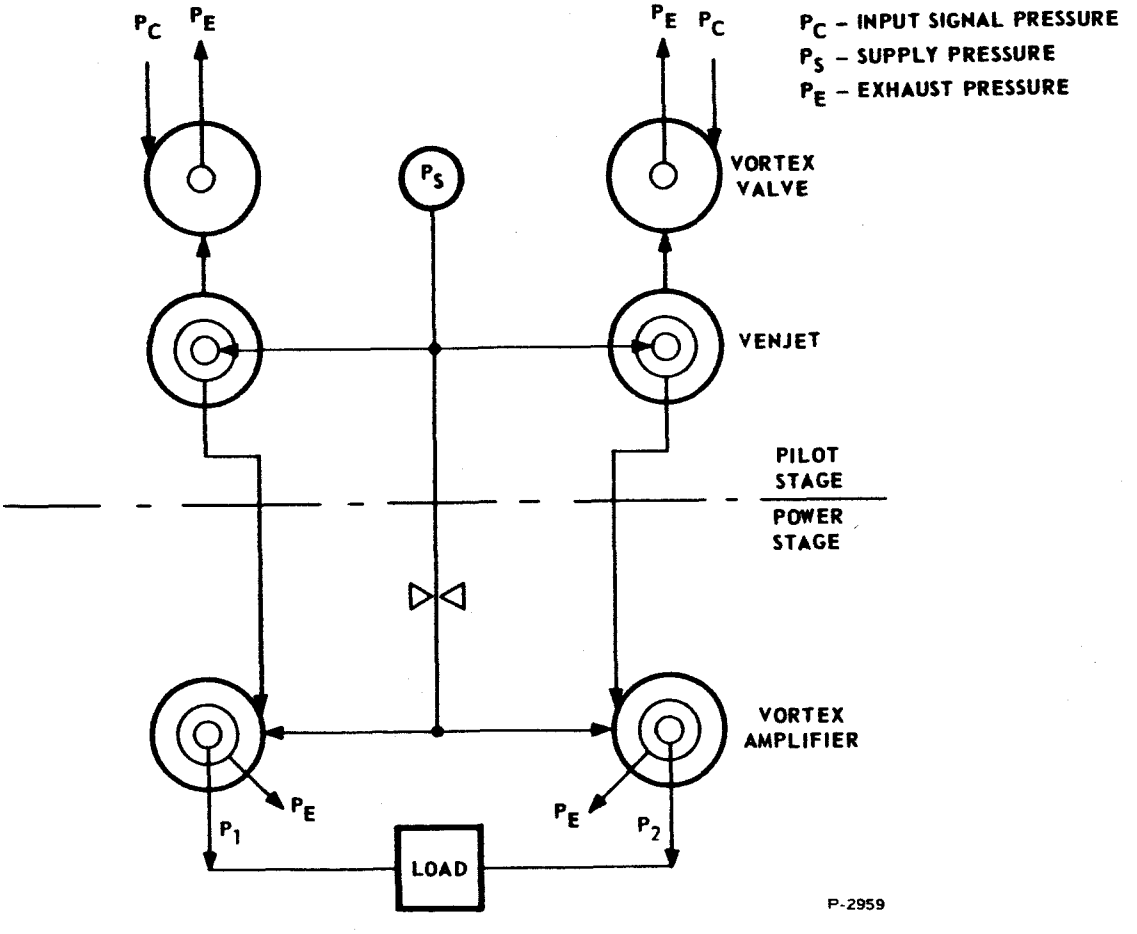

Figure 3-1 - Schematic of Fluid Interaction Servovalve

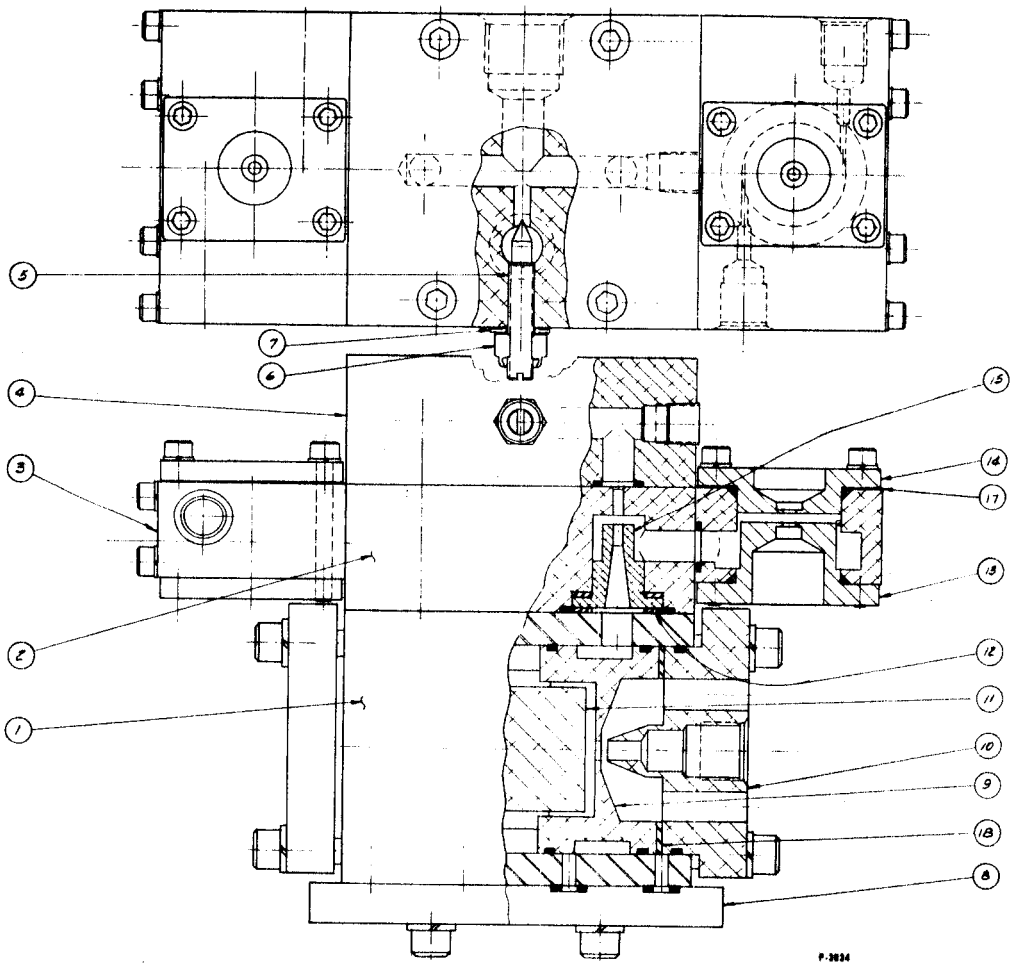

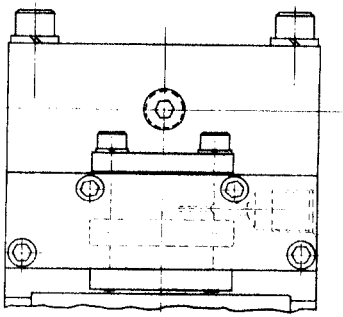

AS REQ'D						
AS REQ	B	2156812	SPACER			16
AS REQ	B	2157538	SHIM			17

AS REQ'D		STOCK	SCREWS & O-RINGS AS REQ'D			14
2	B	2157251	NOZZLE			15
2	C	2157255	CAP-TOP			14
2	C	2157256	CAP-BOTTOM			13
AS REQ'D	B	2157259	SHIM			12
1	C	2156036	CENTER BUTTON			11
2	B	2157100	RECEIVER			10
2	B	2156911	ORIFICE PLATE			9
1	D	2156199	CAP			8
1		STOCK	DYNA-SEAL	PRECISION RUDDER #110-16		7
4		STOCK	HEX NUT 1/4-28NF-3	ESNA #7924-048		6
1	B	2157252	ADJUSTMENT SCREW			5
1	D	2157249	MANIFOLD			4
2	C	2157254	HOUSING			3
1	D	2157248	HOUSING, PILOT VALVE			2
1	D	2156037	HOUSING			1
QTY REQ'D	DWG SIZE	PART NO.	DESCRIPTION	MATERIAL DESCRIPTION & SPECIFICATION	CODE IDENT	ITEM NO.

LIST OF MATERIAL

Figure 3-2 - Assembly Drawing of Servovalve

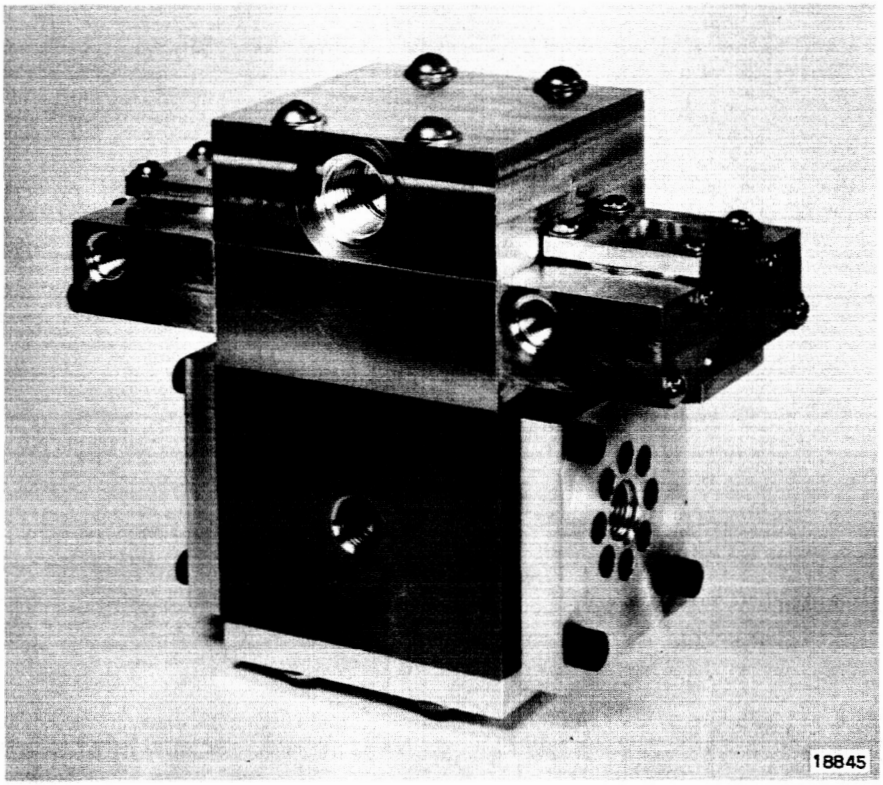

Figure 3-3 - Fluid Interaction Pneumatic Servovalve

implement the servovalve are the vortex valve, vortex pressure amplifier, and Venjet amplifier. Descriptions of these devices and of the pilot and power stage follow.

3.1 FLUID INTERACTION DEVICES

3.1.1 Vortex Valve

The basic vortex valve consists of a cylindrical chamber with supply flow and control flow inlets and an outlet orifice as illustrated in Figure 3-4. The supply flow of gas enters the chamber and, in the absence of control flow as indicated in Figure 3-4(a), proceeds radially inward without resistance and then flows out of the outlet orifice. In the absence of control flow the maximum total flow through the valve is achieved, with the main pressure drop occurring across the outlet orifice. The chamber pressure is slightly less than the supply pressure. Control flow, caused by the control pressure being

above the chamber pressure, is injected tangentially into the chamber, as shown in Figure 3-4(b). The tangential control flow imparts a rotational component to the supply flow. The combined flow has both a tangential and a radial component. The conservation of momentum requires that the tangential velocity and the angular velocity both increase as the flow moves inward. The centrifugal force due to the fluid rotation results in a radial pressure gradient. For a constant supply pressure, this drop in pressure across the chamber reduces the pressure differential across the outlet orifice, and thus reduces the outlet flow.

The vortex valve used in this particular application has two outlet orifices on opposite sides of the vortex chamber, as shown in Figure 3-5. The ratio between maximum and minimum output flow of a dual exit valve is 70 to 90 percent higher than a single exit valve. The normalized performance characteristics of a dual exit valve of

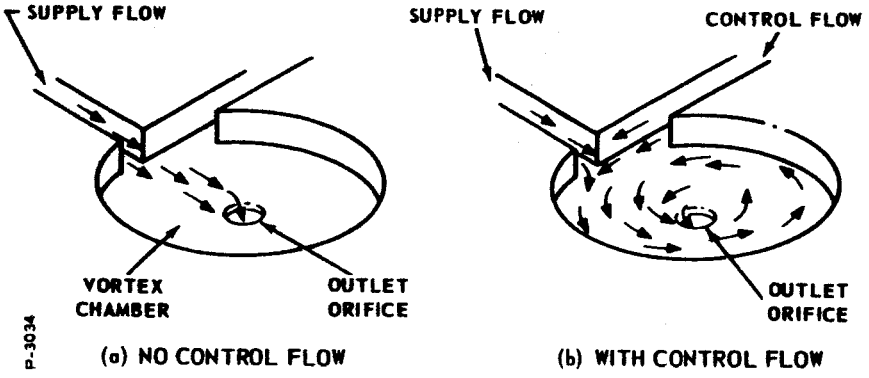

Figure 3-4 - Vortex Valve

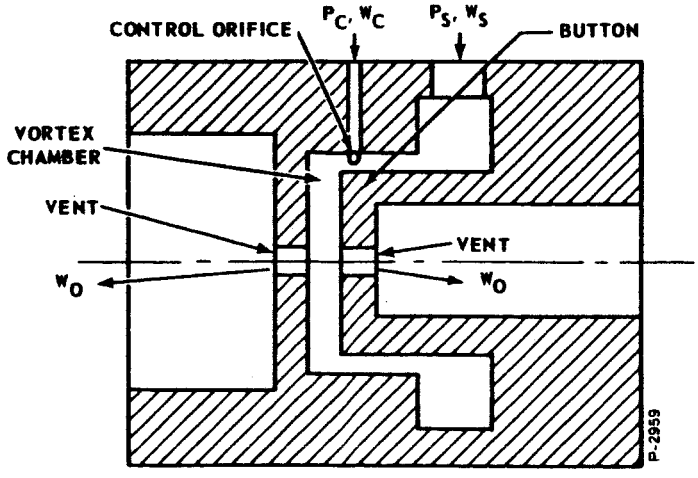

Figure 3-5 - Dual Exit Vortex Valve

approximately the same size as that used in the servovalve are shown in Figure 3-6.

3.1.2 Vortex Pressure Amplifier

A vortex pressure amplifier is similar to a vortex valve with the exception that a pickoff or receiver is placed in the gas stream of the outlet orifice; the pickoff acts in much the same manner as a pitot tube. The receiver pressure and flow is the output of the device. When there is no control flow, the flow out of the outlet orifice is directed into the receiver, Figure 3-7(a), and the pressure and flow recovered under the condition is at a maximum. As control flow is added, the exit flow fans out as shown in Figure 3-7(b) and the recovered pressure decreases. Hence, the vortex pressure amplifier uses the combined effects of the vortex valve and flow diversion for obtaining amplification.

3.1.3 Venjet Amplifier

The Venjet amplifier consists of a nozzle and receiver enclosed in a chamber, as illustrated in the schematic of Figure 3-8. The receiver output pressure and flow vary as functions of the chamber pressure, as shown in Figure 3-9.

In the test from which this data was derived, the Venjet supply pressure was 5.16×10^5 N/m^{2}g (75 psig). The receiver load was the control port of the vortex pressure amplifiers used in the servovalve power stage. The supply pressure to this power stage element was held constant at 3.44×10^5 N/m^{2}g (50 psig). The chamber pressure of the Venjet was controlled by restricting the flow out of the chamber with a hand valve.

The Venjet enables a high output pressure to be controlled by a low vent pressure, which, in turn, can be easily controlled with a vortex valve. The control pressure of the vortex valve need be only slightly above that of the vent pressure. The Venjet is therefore well suited for controlling the high control pressure of the power stage vortex devices.

3.2 PILOT STAGE

The pilot stage consists of two Venjets controlled by dual exit vortex valves. One Venjet and vortex valve combination is shown in Figure 3-10. The supply pressure to the Venjet is the 5.16×10^5 N/m^{2}g (75 psig) supply to the servovalve.

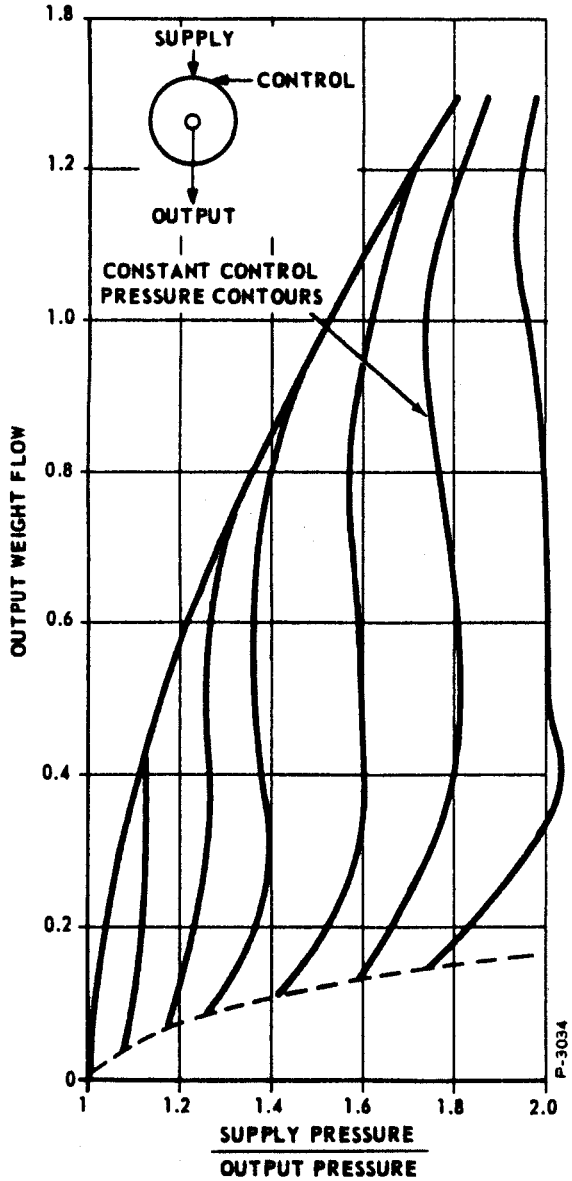

Figure 3-6 - Normalized Characteristic Curves for Dual Exit Vortex Valve

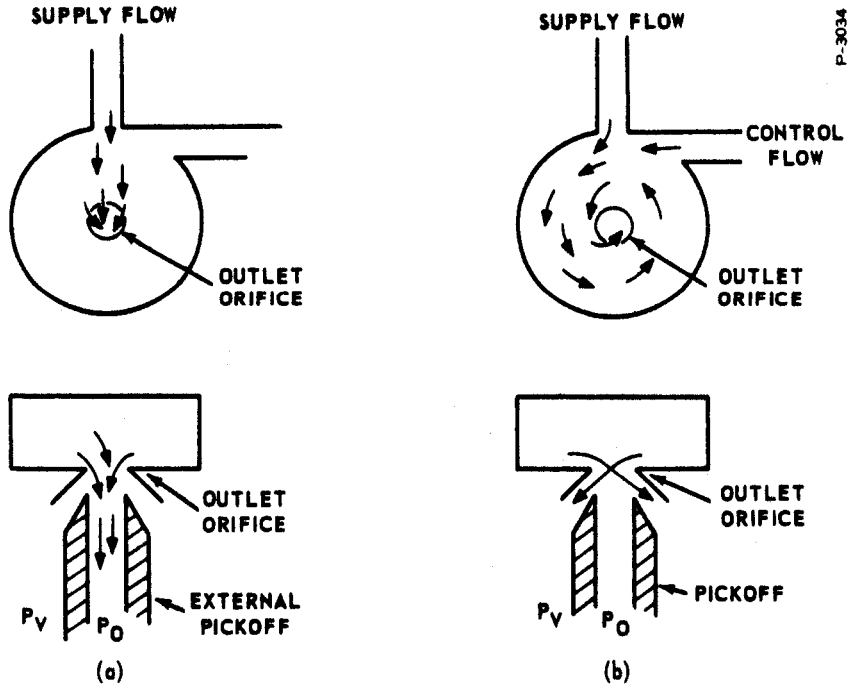

Figure 3-7 - Vortex Amplifier

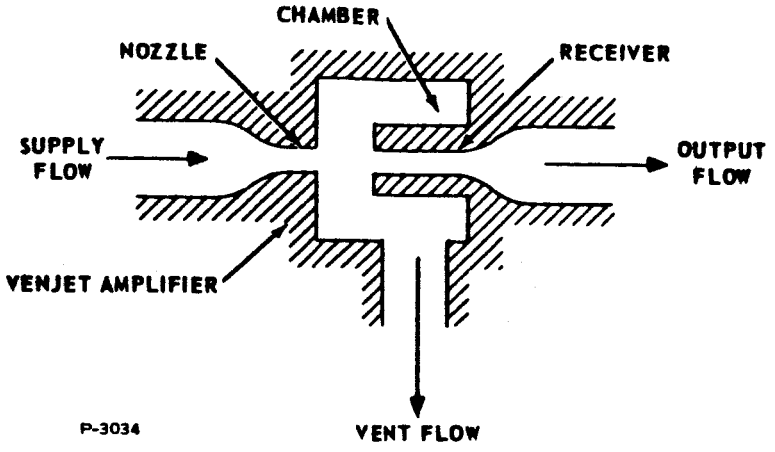

Figure 3-8 - Schematic of Venjet Amplifier

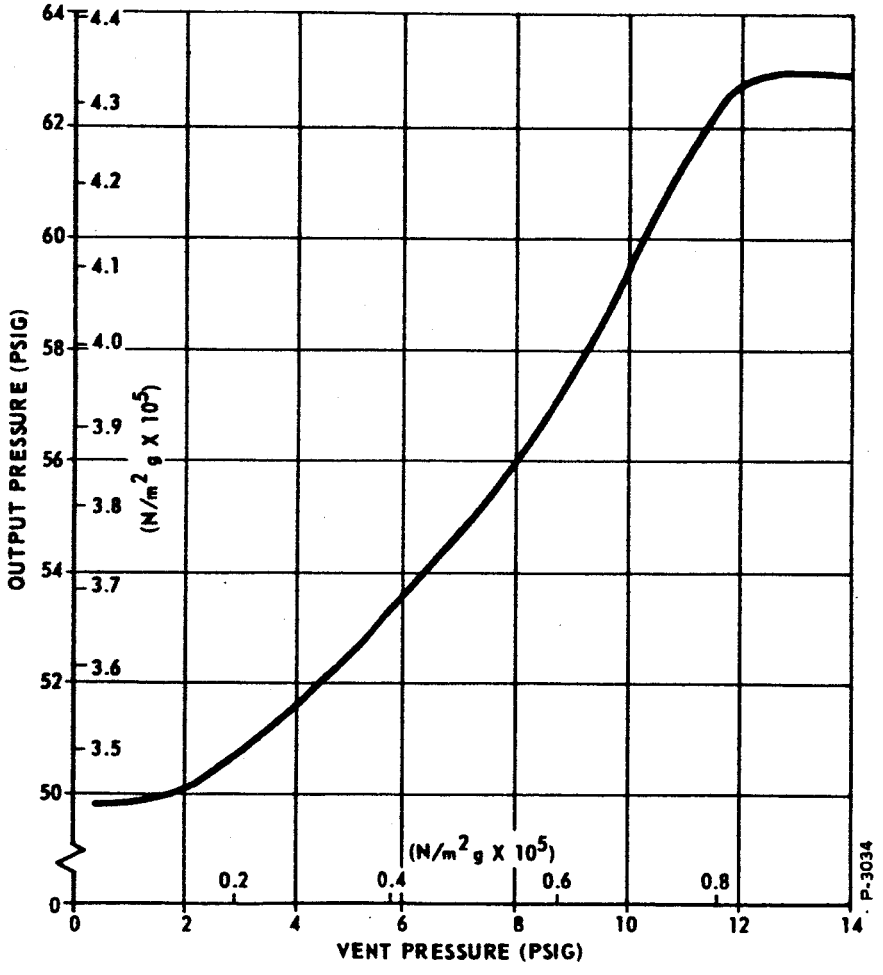

Figure 3-9 - Output Pressure Vs. Vent Pressure of Pilot Stage Venjet

The output of the Venjet is the control signal to one of the power stage vortex pressure amplifiers, and the flow out of the Venjet chamber (vent flow) is controlled by a dual exit vortex valve that acts as a variable restriction. The control flow to the dual exit vortex valve is one of the input signals to the servovalve.

The effective orifice size of the vortex valve is a function of the pressure differential between the Venjet chamber pressure and the control input signal to the servovalve. The control signal to the vortex valve need only be slightly higher than the chamber pressure to restrict the chamber vent flow. The operation of the dual exit vortex valve in combination with the Venjet is illustrated graphically in Figure 3-11. In this figure the valve characteristics of Figure 3-6 are shown with a load line along which the valve would operate when used in combination with a Venjet. The Venjet chamber pressure is the supply pressure of the vortex valve, and the valve supply flow is the vent flow of the Venjet. As the control input pressure to the vortex valve increases, the vent flow from the Venjet chamber decreases and the Venjet chamber pressure increases, causing the Venjet receiver pressure and flow to increase.

In this application the ratio between the Venjet chamber pressure and the Venjet supply pressure is always less than the critical pressure ratio, and the Venjet supply pressure is constant. Therefore the Venjet supply flow is constant.

The significant dimensions of the pilot stage components are as follows:

Venjet Valve

Nozzle diameter	0.249 cm (0.098 in.)
Receiver diameter	0.249 cm (0.098 in.)
Nozzle to receiver spacing	0.262 cm (0.103 in.)

Vortex Valve

Vortex chamber diameter	2.54 cm (1.00 in.)
Vortex chamber length	0.369 cm (0.156 in.)
Vortex chamber outlet diameter	0.450 cm (0.177 in.) (button side) 0.457 cm (0.180 in.) (opposite side)
Button diameter	2.22 cm (0.877 in.)
Control orifice diameter (Single Orifice)	0.140 cm (0.055 in.)

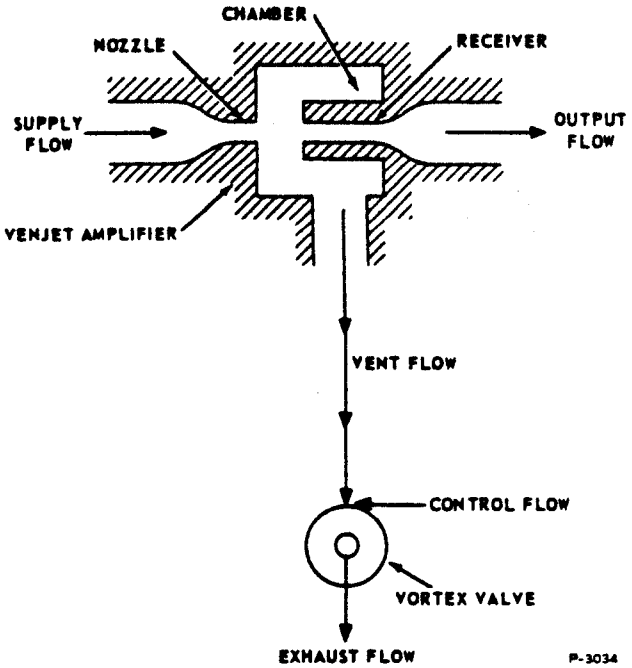

Figure 3-10 - Schematic of Pilot Stage

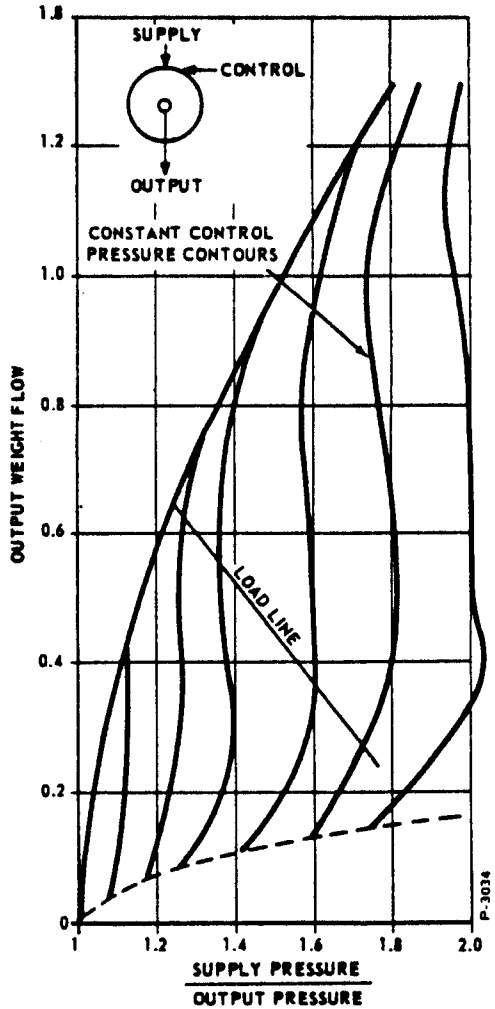

Figure 3-11 - Normalized Characteristic Curves for Dual Exit Vortex Valve with Venjet Load Line

3.3 POWER STAGE

The power stage, shown schematically in Figure 3-12, is composed of two vortex pressure amplifiers which are operated in push-pull and produce a pressure flow characteristic similar to the conventional four-way bridge, spool type servovalve. An increase of control pressure P_{C1} diverts the flow leaving the output orifice of valve V_1 and thereby reduces the recovered pressure P_1. A simultaneous reduction of P_{C2} converges the flow leaving V_2 to increase P_2. The result is a differential pressure $P_2 - P_1$ across the load.

When the two valves are operated to drive an actuator load, it is necessary for one valve to absorb reverse flow from the actuator when the load is moving. The vortex amplifier receiver is designed to provide this type of operation. With the outlet flow at a minimum value and fully diverted to exhaust, the backflow is exhausted with minimum back pressure by providing sufficient area between the valve and receiver.

An orifice in the supply line to the power stage drops the pressure from 5.16 N/m^2g (75 psig) to about 3.58×10^5 N/m^2g (52 psig). The quiescent control pressures to the power stage are set at a value that results in a quiescent supply flow to each vortex pressure amplifier equal to one-half of the maximum supply flow to the power stage. When

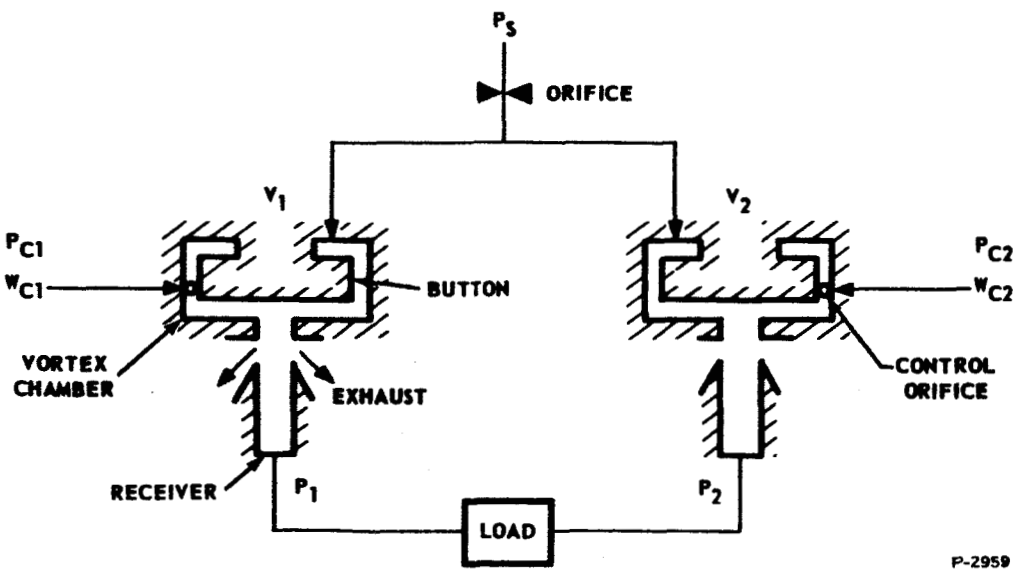

Figure 3-12 - Schematic of Power Stage of Fluid Interaction Servovalve

the control pressures are varied about the quiescent condition by an input signal to the valve, one control pressure to the power stage increases and the other decreases. This change in control pressures results in an increase in supply flow to one vortex pressure amplifier and a decrease in the supply flow to the other. Also, the supply flow to each vortex pressure amplifier is almost independent of the receiver load or output flow. Thus the supply flow to the power stage and consequently the supply pressure, which is the drop through the orifice, remain relatively constant.

The pressure-flow characteristics of the vortex amplifier are shown in Figure 3-13. The forward flow curve indicates the pressure flow characteristic in the receiver-to-load direction with no control flow in the vortex chamber. The reverse flow curve illustrates the pressure-flow characteristic in the load-to-receiver direction with maximum control flow to the vortex chamber. The two curves can be used to determine the load pressure-flow characteristics of the power stage with a variable orifice load. The maximum no-load flow is determined by the point of intersection of the curves. The differential load pressure at a given load weight flow is found by subtracting the corresponding pressures. This procedure was performed graphically, and the resulting load pressure-flow characteristic is shown in Figure 3-14.

The data in Figure 3-13 was taken with a supply pressure of 3.44×10^5 N/m^{2}g (50 psig). The maximum blocked load pressure recovery is 3.24×10^5 N/m^2 (47 psi) or 0.94 of supply pressure; the maximum no-load flow recovery is 0.69 of the total flow. The ratio of maximum control weight flow to load weight flow is 0.26.

The significant dimensions of the vortex amplifier are as follows:

Vortex chamber diameter	3.300 cm (1.300 in.)
Vortex chamber length	0.236 cm (0.093 in.)
Control orifice diameter (five orifices)	0.119 cm (0.047 in.)
Vortex chamber outlet orifice diameter	0.470 cm (0.185 in.)
Button diameter	3.060 cm (1.207 in.)
Vortex chamber outlet to receiver length	0.165 cm (0.065 in.)
Receiver orifice diameter	0.493 cm (0.194 in.)

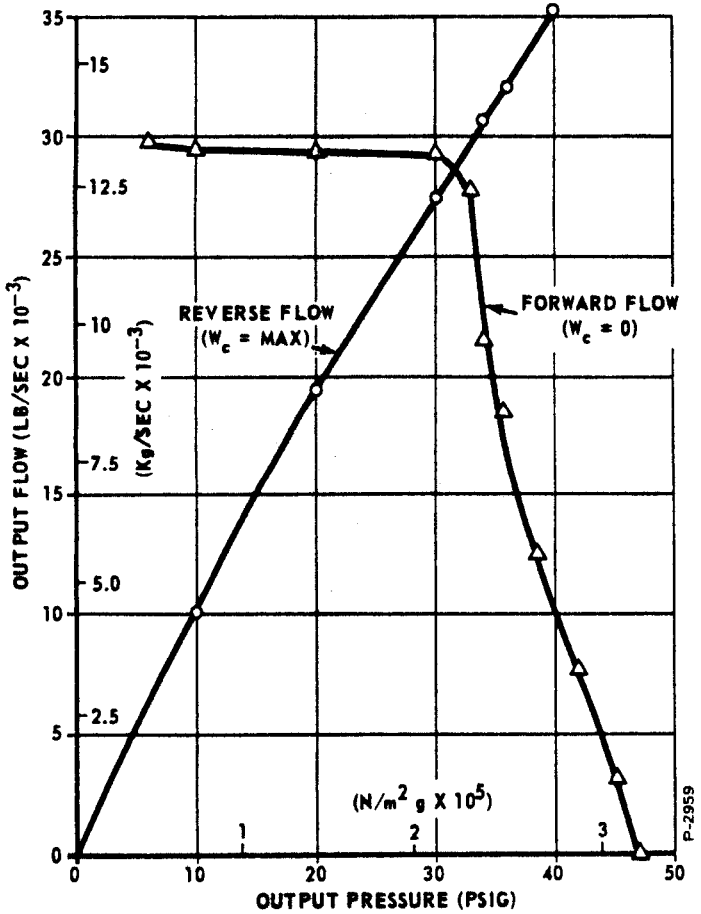

Figure 3-13 - Pressure-Flow Characteristic for a Vortex Amplifier

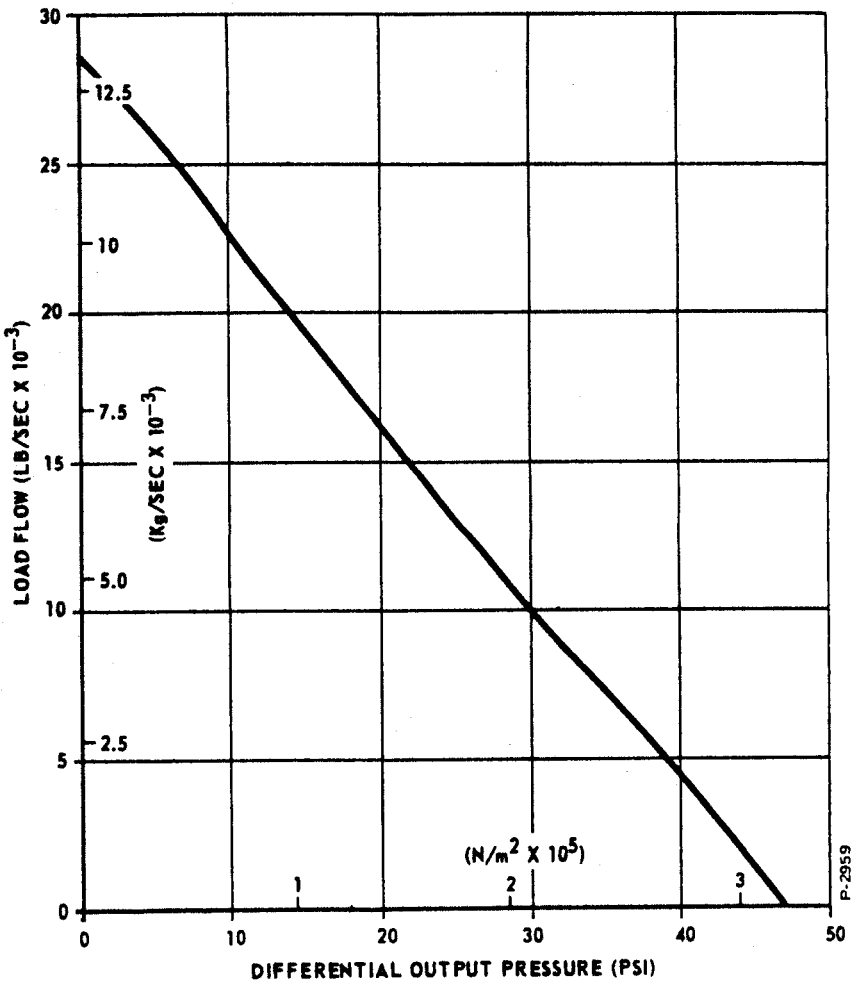

Figure 3-14 - Load Flow Vs. Differential Output Pressure

SECTION 4

SERVOVALVE ACCEPTANCE TEST

4.1 TEST OBJECTIVE

The objective of the acceptance test was to establish the conformance of the fluid interaction servovalve performance to that specified. The servovalve specifications are listed in Appendix A.

4.2 TEST EQUIPMENT

The transient response, threshold, output stability, hysteresis, and symmetry tests were conducted using the test setup shown schematically in Figure 4-1. A Bendix Model Number 356, four-way, closed center, electropneumatic servovalve was used to vary the input control pressures. The electropneumatic servovalve was controlled by a servo amplifier, and the input signal was varied either manually or by a function generator. The differential output and input pressures to the fluid interaction servovalve were measured by means of differential pressure transducers. The pressures were recorded on the X-Y plotter or by photographing the oscilloscope trace. The pressure transducers were calibrated using a master pressure gauge. A calibration check of the master pressure gauge with a dead weight tester showed the gauge to be accurate within ±0.5 percent.

Tests of input admittance, of input signal pressure and flow versus differential output pressure, and of output flow versus differential output pressure were conducted using the test setup as shown in Figure 4-2. For these tests, rotameters were used to measure input, control, and load flows, and pressure gauges were used to measure pressures. Figure 4-3 shows a photograph of the test setup.

The load volumes used in the stability tests were measured by filling them with a measured quantity of water. The load volumes were all found to be about 4.9 cm^3 (0.3 $in.^3$) larger than the calculated or nominal value. The specified filter $\left|\frac{1}{(0.05S + 1)^2}\right|$ for filtering the differential output pressure of the valve in the stability tests was checked by measuring the output versus frequency with a scope and function generator. The amplitude ratio versus frequency is shown in Figure 4-4

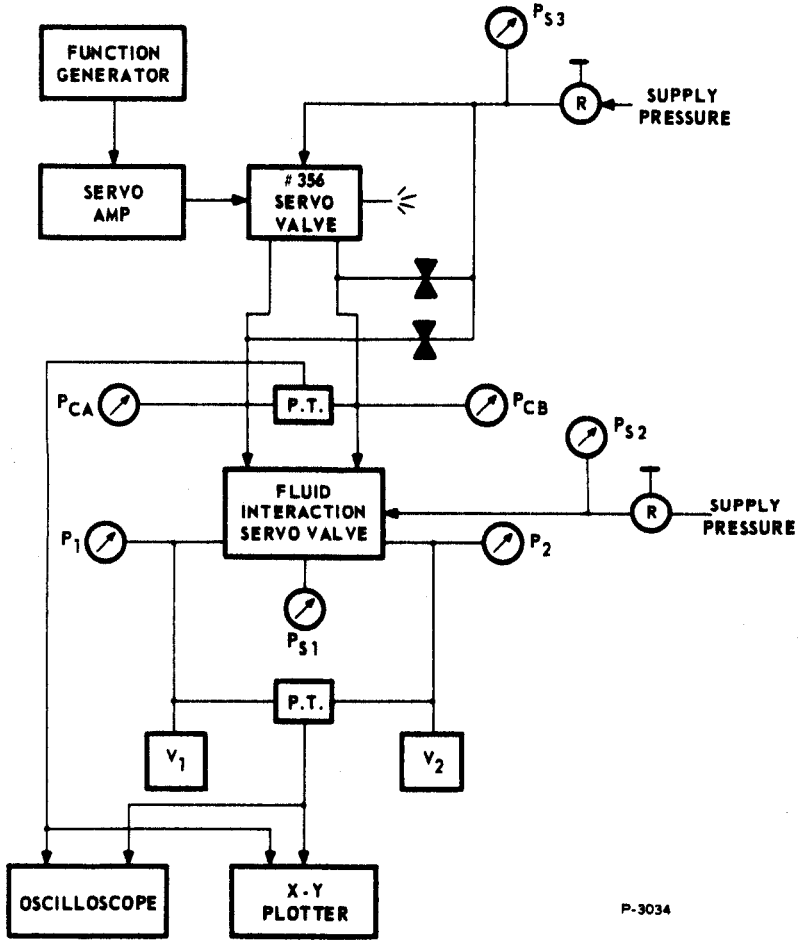

Figure 4-1 - Fluid Interaction Servovalve Test Setup No. 1

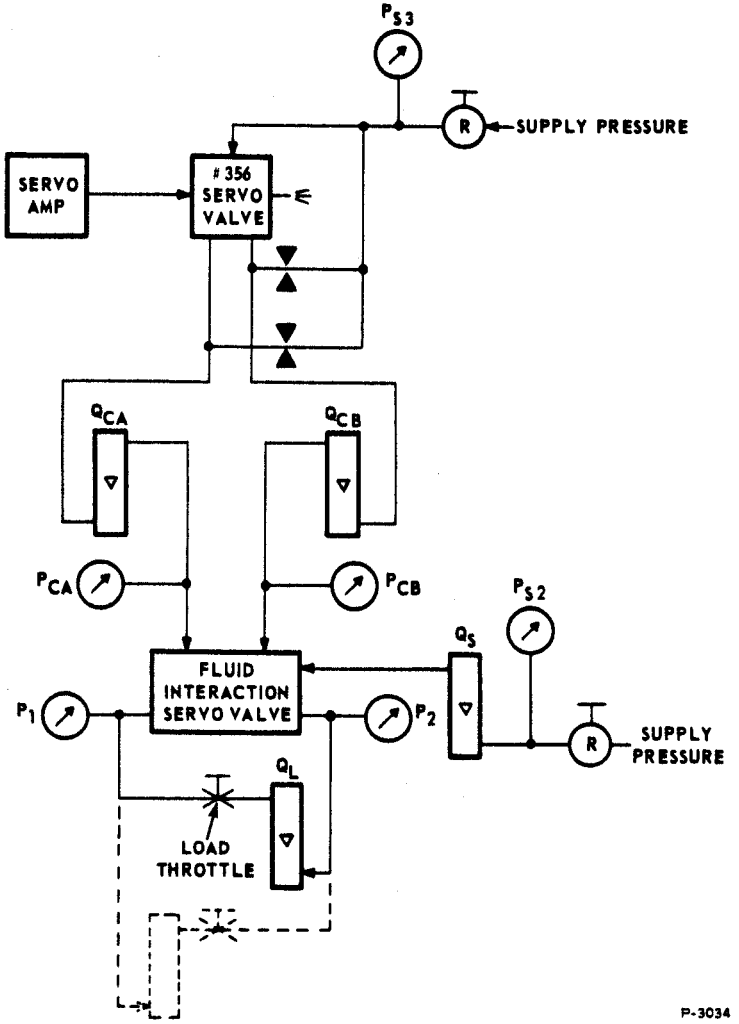

Figure 4-2 - Fluid Interaction Servovalve Test Setup No. 2

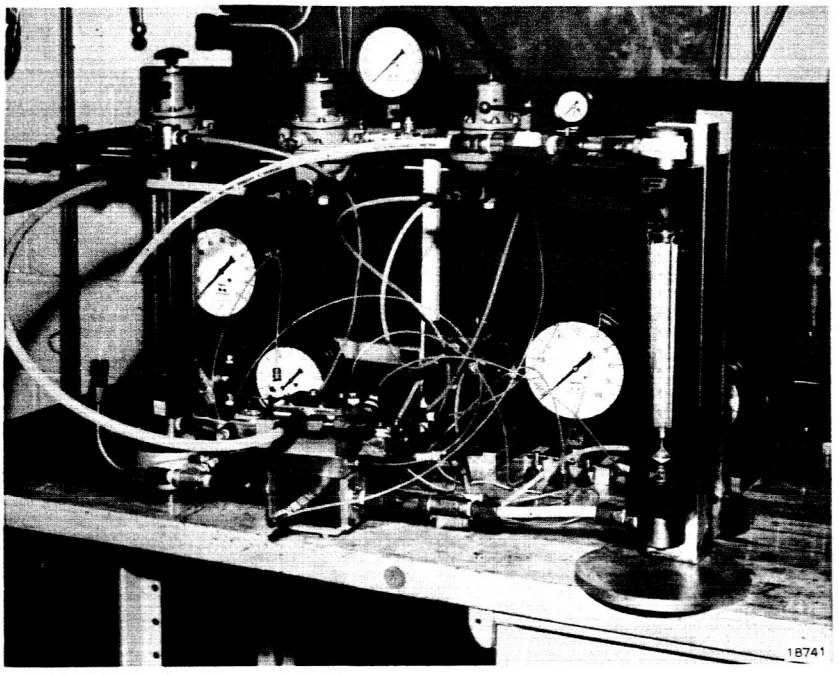

Figure 4-3 - Photograph of Servovalve Test Setup

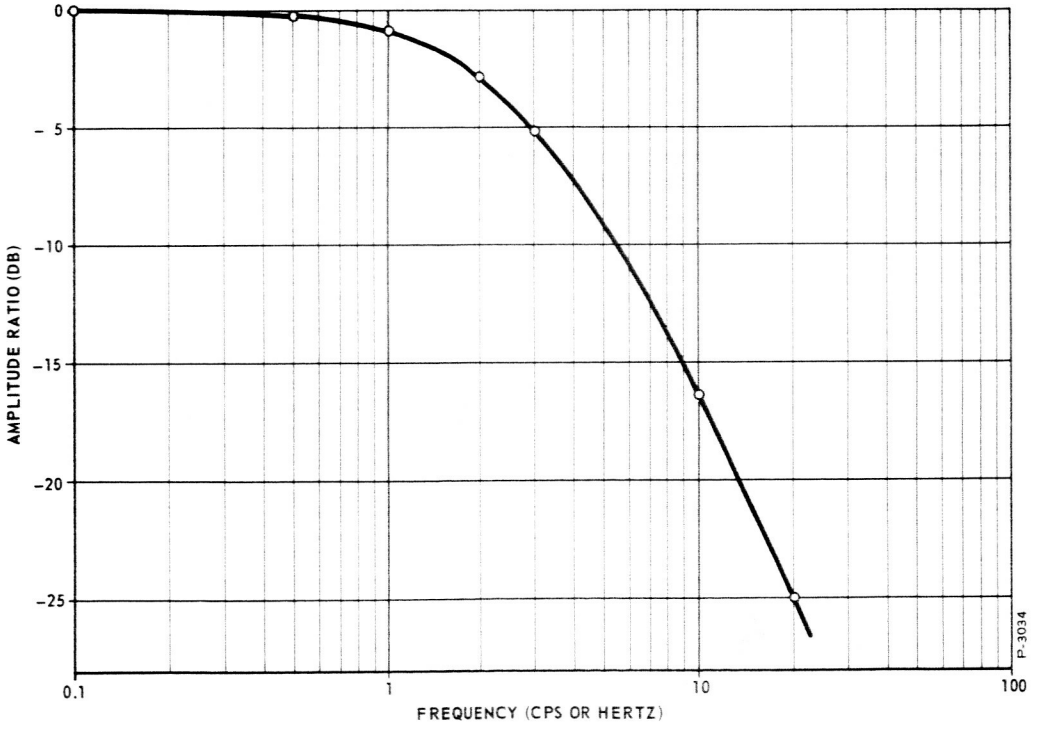

Figure 4-4 - Frequency Response of Filtered Pressure Transducer Output Circuit used in Stability Test

4.3 DETAILED TEST PROCEDURE

For all tests, the supply pressure to the servovalve was set at 5.16×10^5 N/m^2 g (75 psig).

4.3.1 Transient Response

The transient response of the valve was established by introducing a step input signal into the valve which resulted in a 0.69×10^5 N/m^2 (10 psi) change in the differential output pressure, and by recording both the input and output pressures as a function of time.

Detailed Procedure

(a) Set up equipment as shown in Figure 4-1.

(b) Set sweep time of the oscilloscope at 0.1 sec/cm.

(c) Set vertical sensitivity of the oscilloscope to 0.172×10^5 N/m^2/cm (2.5 psi/cm) for both input and output pressures.

(d) Apply step input signal at 1 cps with 0.69×10^5 N/m^2 (10 psi) change in differential output pressure. Close load throttle.

(e) Photograph simultaneous traces of differential input signal ($P_{CA} - P_{CB}$) and differential output signal ($P_1 - P_2$).

4.3.2 Threshold

The threshold of the valve was established by recording the input and output differential pressures as a function of time with a sine wave input. The input signal amplitude was gradually decreased until the output no longer followed the input.

Detailed Procedure

(a) Set sweep time of the oscilloscope at 1 sec/cm.

(b) Place the $\frac{1}{(0.05S + 1)^2}$ filter in output pressure circuit.

(c) Set vertical sensitivity of scope to 0.086×10^5 $N/m^2/cm$ (1.25 psi/cm) for both input and output pressures.

(d) Photograph simultaneous traces of differential input signal ($P_{CA} - P_{CB}$) and differential output signal ($P_1 - P_2$) with smallest discernible regular movement of output trace.

4.3.3 Output Stability

The output stability was measured by recording the output differential pressure versus time with a constant input signal. This test was performed with closed load throttle and with various combinations of load volume sizes and input signals. The load volumes used were: (1) V_1 equal to 139 cm^3 (8.5 in^3), V_2 equal to 24.6 cm^3 (1.5 in^3); (2) V_1 and V_2 equal to 82 cm^3 (5 in^3); and (3) V_1 equal to 24.6 cm^3 (1.5 in^3, V_2 equal to 139 cm^3 (8.5 in^3).

Detailed Procedure

(a) Set sweep time of scope at 0.2 sec/cm.

(b) Set vertical sensitivity of scope to 0.086×10^5 $N/m^2/cm$ (1.25 psi/cm) for the output differential pressure.

(c) Leave load throttle closed. Set $V_1 = V_2 = 82\ cm^3 (5\ in^3)$.

(d) Photograph trace of differential output signal with input signal set such that ($P_1 - P_2$) equals 0, $\pm 1.03 \times 10^5$ N/m^2, $\pm 2.06 \times 10^5$ N/m^2, and $\pm 3.1 \times 10^5$ N/m^2 (0, ±15, ±30, and ±45 psi).

(e) Adjust load volumes such that V_1 = 139 cm^3 (8.5 in^3) and V_2 - 24.6 cm^3 (1.5 in^3).

(f) Photograph trace of differential output signal with input signal set such that ($P_1 - P_2$) equals 0, and $\pm 1.03 \times 10^5$ N/m^2 (±15 psi).

(g) Adjust load volumes such that V_1 = 24.6 cm^3 (1.5 in^3) and V_2 = 139 cm^3 (8.5 in^3).

(h) Repeat (f).

4.3.4 Hysteresis and Symmetry

The differential output pressure was recorded as a function of the differential input pressure on an X-Y plotter as the input signal varied slowly from plus to minus and back to plus rated input signal.

Detailed Procedure

(a) Connect input and output differential pressure transducers to the X-Y plotter. The output differential pressure is connected to the Y axis input with a sensitivity of 10 psi/inch. The input differential pressure is connected to the X axis input with a sensitivity of 5 psi/inch.

(b) Vary the input signal from plus to minus rated input signal by means of a 0.01 cps triangular wave input signal. Plot one complete cycle.

4.3.5 Input Pressure and Flow Versus Differential Output Pressure

The control input pressures and flows and output pressures were recorded at various input signal levels with closed load throttle.

Detailed Procedure

(a) Set up equipment as shown in Figure 4-2.

(b) Record input pressures P_{CA} and P_{CB}, output pressures P_1 and P_2, and input flows Q_{CA} and Q_{CB} at output differential pressures of 0, $\pm 1.03 \times 10^5$ N/m^2, $\pm 2.06 \times 10^5$ N/m^2, and $\pm 3.1 \times 10^5$ N/m^2 (0, ± 10, ±25, ±40 and ±45 psi).

4.3.6 Input Admittance

The input admittance of the valve was established by recording the control input pressures and flows and the load flow for various throttle openings with a constant input signal.

Detailed Procedure

(a) Close load throttle. Set $P_1 - P_2 = 1.52 \times 10^5$ N/m^2 (22 psi).

(b) Record input pressures P_{CA} and P_{CB} and input flows Q_{CA}, Q_{CB} and Q_L.

(c) Open load throttle wide open. Repeat (b).

(d) Close load throttle such that Q_L equals half of Q_L recorded in (c). Repeat (b).

(e) Close load throttle. Set $P_1 - P_2 = 3.1 \times 10^5$ N/m^2 (45 psi). Repeat (b).

(f) Open load throttle wide open. Repeat (b).

(g) Close load throttle such that Q_L equals half of Q_L recorded in (f). Repeat (b).

4.3.7 Output Flow Versus Differential Output Pressure

The differential output pressure, load flow and supply flow were recorded with various settings of the load throttle with constant input signal.

Detailed Procedure

(a) Record differential output pressure ($P_1 - P_2$) and flows Q_L and Q_{S1} with 100 percent rated input signal and with various settings of the load throttle from closed to open. Take readings at intervals of 0.34×10^5 N/m^2 (5 psi) differential output pressure.

(b) Repeat with reversed output flow.

(c) Repeat (a) and (b) with input set such that closed load throttle differential pressure equals 0.69×10^5 and 1.38×10^5 N/m^2 (10 and 20 psi).

4.4 ACCEPTANCE TEST RESULTS

4.4.1 Summary and Discussion of Results

The servovalve test and performance is compared with the specified requirements in Table 4-1. The measured performance met or exceeded specified requirements in a majority of the items compared. Measured performance did not meet specifications in five cases, namely,

quiescent supply flow, input signal power, flow recovery, output stability, and linearity. These cases are discussed below.

The quiescent supply flow, input signal power, and flow recovery can be improved by merely optimizing the size of pilot and power stages. Both the pilot stage and power stage are slightly oversize, and the quiescent supply flow, flow recovery, and power input performance would more closely match the requirements if the valve were sized more exactly. The rated no-load output flow is 0.0131 Kg/sec (0.029 pps) which

Table 4-1 - Comparison of Measured Performance of the Fluid Interaction Servovalve with Specified Requirements

Item *	Specified	Measured
3. Supply Pressure	5.16×10^5 N/m^{2}g air (75 psig)	5.16×10^5 N/m^{2}g air (75 psig)
4. 1 Load	$V_C - V_D \leq 115$ cm^3 (7 in.^{3}) $V_C + V_D = 164$ cm^3 (10 in.^{3})	$V_C - V_D \leq 115$ cm^3 (7 in.^{3}) $V_C + V_D = 164$ cm^3 (10 in.^{3})
5. 2 Input Signal Pressure	2.75×10^5 N/m^{2}g max (40 psig)	1.72×10^5 N/m^{2}g (25 psig)
5. 3 Input Signal Bias	1.38×10^5 N/m^{2}g max (20 psig)	1.17×10^5 N/m^{2}g (17 psig)
5. 4 Input Signal Power	30 watts max.	55 watts
5. 5 Input Admittance	10% max.	2%
6. Quiescent Supply Flow	0.0204 Kg/sec max (0.045 pps)	0.030 Kg/sec (0.067)
7. Rated No-Load Output Flow	0.0113 Kg/sec (0.025 pps)	0.0131 Kg/sec (0.029 pps)
8. Flow Recovery	0.55 min	0.44
9. Pressure Recovery	3.1×10^5 N/m^2 min (45 psi)	3.1×10^5 N/m^2 (45 psi)
10. Output Pressure Bias	Not Specified	1.24×10^5 N/m^2 (18 psig)
11. Differential Input Signal Power Change for Output Pressure Change of from -0.69×10^5 to 0.69×10^5 N/m^2 (-10 to +10 psi)	5 watts max	5 watts
12. Linearity	$\frac{\text{Gain max}}{\text{Gain min}} < 3$	15
13. Output Flow vs. Differential Output Pressure	$\geq Q_o \left[1 - \frac{P}{P_0}\right]$	$\geq Q_o \left[1 - \frac{P}{P_o}\right]$
14. Output Stability	0.034×10^5 N/m^2 max (0.5 psi)	0.27×10^5 N/m^2 (4 psi)
15. Transient Response	0.25 sec	0.10 sec
16. Symmetry	γ max - γ min <0.2 γ max	γ max - γ min = 0.02γ max
17. Threshold	0.5% max	0.5%
18. Hysteresis	3% max	3%
*See Appendix A		

P-3034

is 16 percent higher than the required 0.0113 Kg/sec (0.025 pps). Thus both the power stage and pilot stage could be made smaller and this would decrease the quiescent supply flow. Furthermore the pilot stage was oversized about 15 percent for the present power stage. Decreasing both the pilot stage and power stage to the optimum size would result in a decrease in the quiescent supply flow to 0.0245 Kg/sec (0.054 pps) and an increase in the flow recovery to 0.49. The maximum total input control power would also decrease from 55 watts to about 46 watts.

The non-linearity of the valve is mainly caused by the non-linear flow gain characteristics of the pilot stage vortex valves. The vortex valves require a considerable amount of control flow before they begin to turn down or shut off appreciably. The vortex valve exit orifices are slightly oversize so that decreasing the exit orifices diameters would help the linearity. The vortex valves should also be designed with more linear flow gain characteristics.

The stability of the valve can be improved by decreasing the input control pressure bias. The maximum peak to peak ripple can be decreased to about 0.103 to 0.138×10^5 N/m^2 (1.5 to 2 psi) by this means. However, this modification results in a more nonlinear differential output versus differential input pressure gain curve. Decreasing the volume in the supply line between the pressure dropping orifice and the power stage vortex amplifiers would probably also improve the stability.

4.4.2 Test Performance Data

The output flow versus differential output pressure is shown in Figure 4-5. From this figure it is seen that the maximum pressure differentials with closed load throttle were $+3.10 \times 10^5$ and -3.17×10^5 N/m^2 (+45 and -46 psi). With wide open load throttle the maximum output flows were 0.0137 and - 0.0125 Kg/sec (+0.0303 and -0.0277 pps). The supply flow remained at 0.030 Kg/sec (0.067 pps) during this test under all input and load throttle conditions.

The control input power for each input line versus differential output pressure is shown in Figure 4-6. The differential output pressure versus differential control input power is shown in Figure 4-7. The ratio between maximum and minimum gain is 15. The curve does not quite pass through the origin and is somewhat asymmetrical because of slight orifice size differences between one half of the valve and the other. The shape of the curve can be adjusted somewhat by changing the control input pressure bias level. A lower control input pressure bias

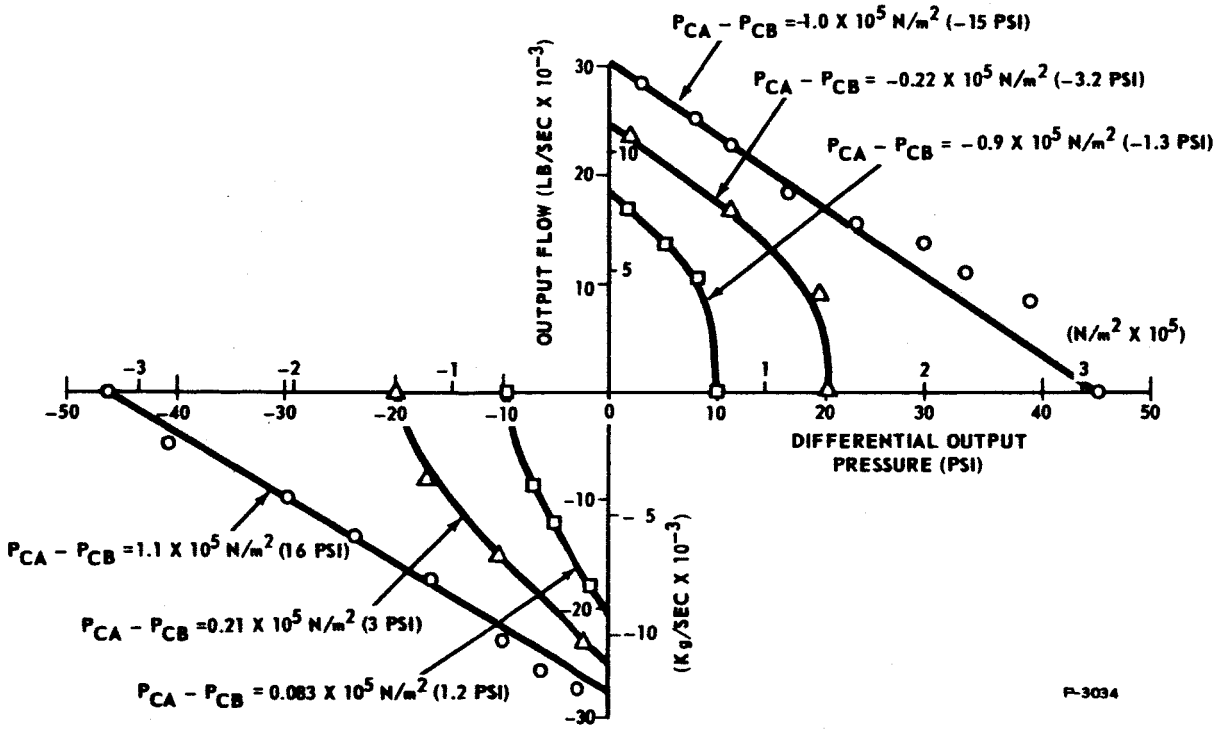

Figure 4-5 - Servovalve Output Flow vs Differential Output Pressure

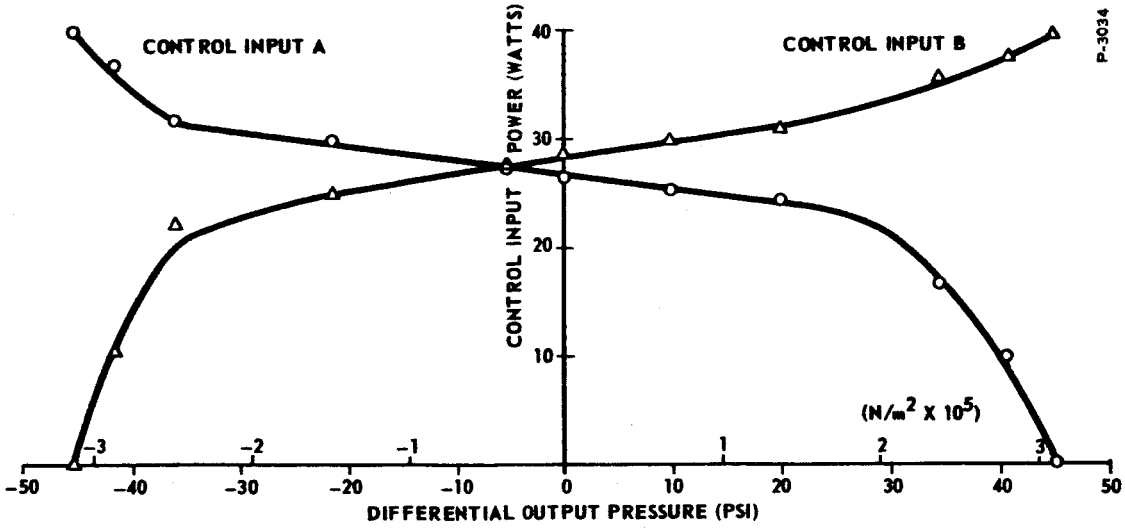

Figure 4-6 - Servovalve Control Input Power vs Differential Output Pressure

level decreases the gain in the center portion of the curve but increases the asymmetry near the ends of the curve. The differential output pressure versus differential control pressure is shown in Figure 4-8. The output pressure versus control pressure curve is similar in shape to the output pressure versus control power curve.

Representative stability data is shown in Figure 4-9. The output differential pressure does not have a regular oscillation but rather seems to have a random variation about a given average differential pressure. A maximum peak to peak variation of 0.27×10^5 N/m^2 (4 psi) was found from data taken with various inputs and combinations of load volumes.

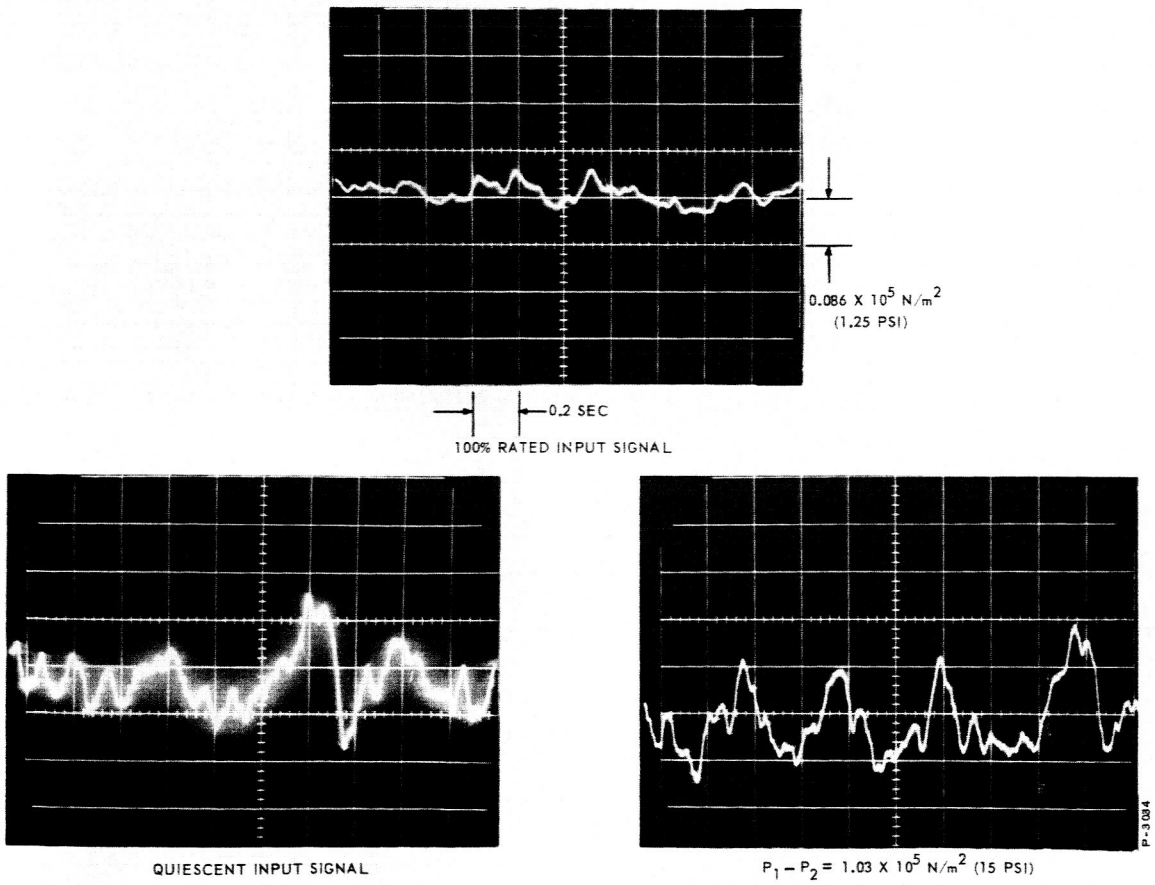

Figure 4-9 - Servovalve Output Differential Pressure Stability

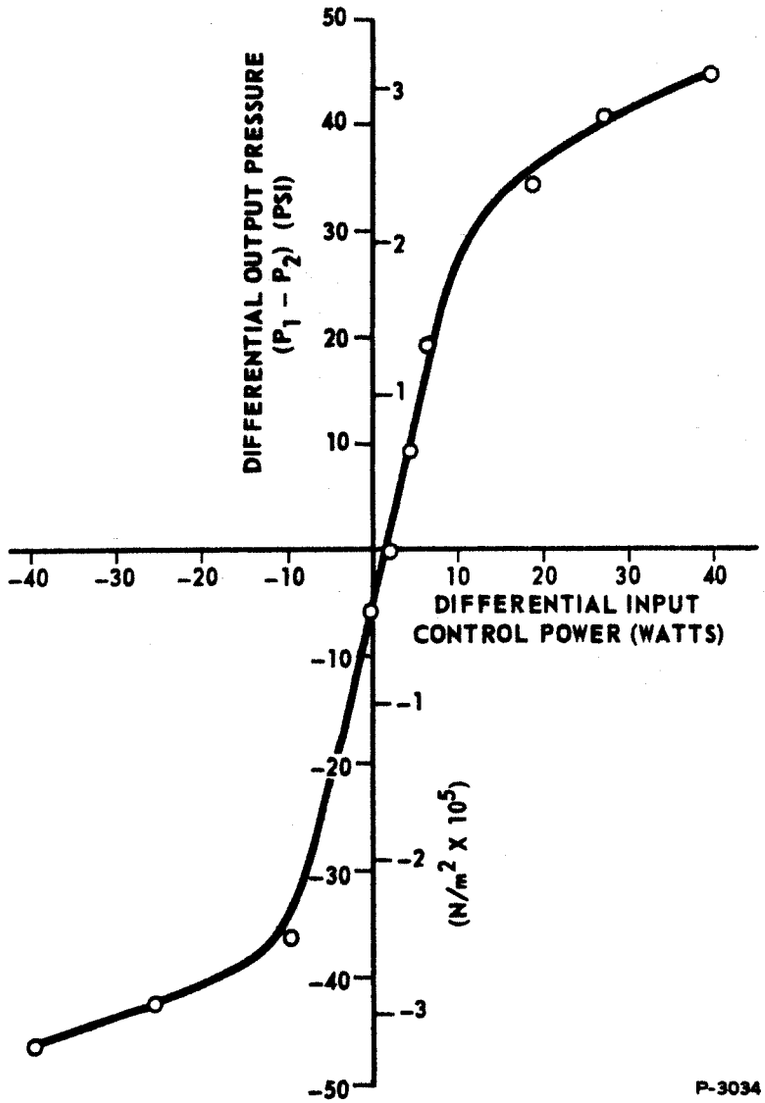

Figure 4-7 - Servovalve Differential Output Pressure vs. Differential Input Power

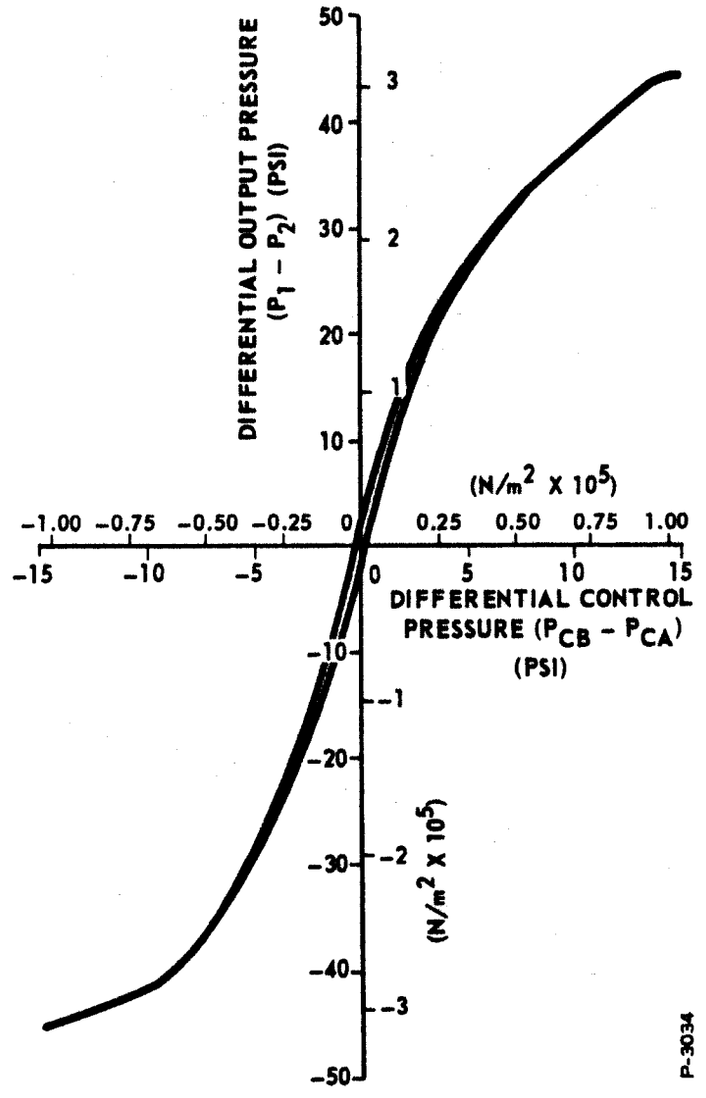

Figure 4-8 - Servovalve Differential Output Pressure vs. Differential Control Power

The transient response is shown in Figure 4-10. The input pressure was not a true step because of the limited transient response of the input electropneumatic servovalve. However, the output pressure followed the input pressure very closely, and the output pressure settled within 0.069×10^5 N/m^2 (1 psi) of the final differential output pressure in a time period of about 0.1 second, which is well under the maximum specified value of 0.25 seconds.

The threshold data is shown in Figure 4-11. The increment of differential input signal power required to produce a change in output was less than 0.5 percent of the difference in the differential input signal power between zero and rated input signal. The threshold of the pneumatic servovalve is probably lower than this but the spool of the input electropneumatic servovalve stopped moving for smaller inputs than that shown in the data.

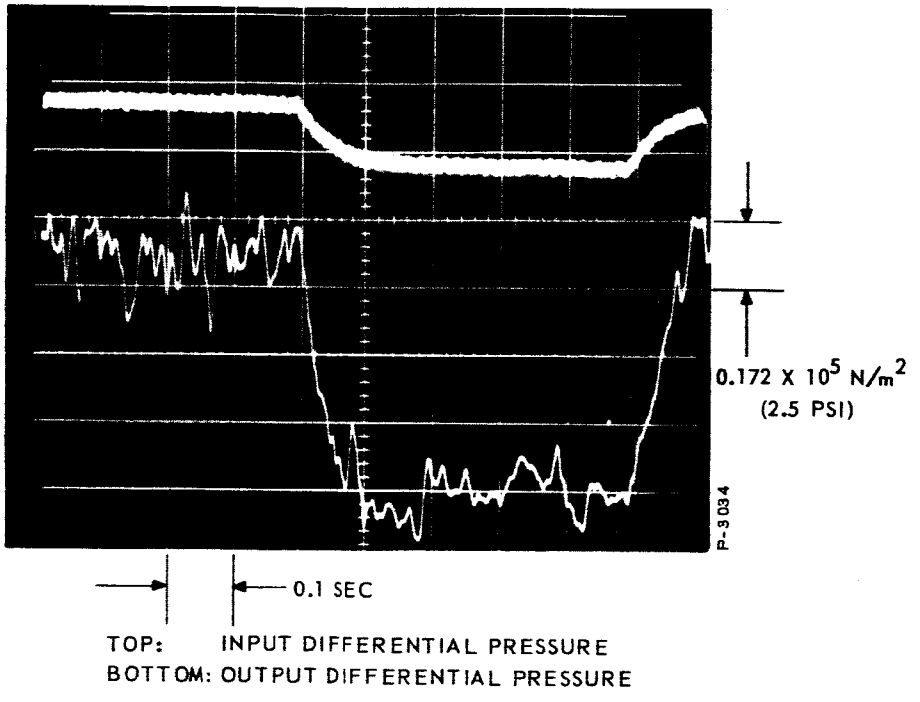

Figure 4-10 - Servovalve Transient Response

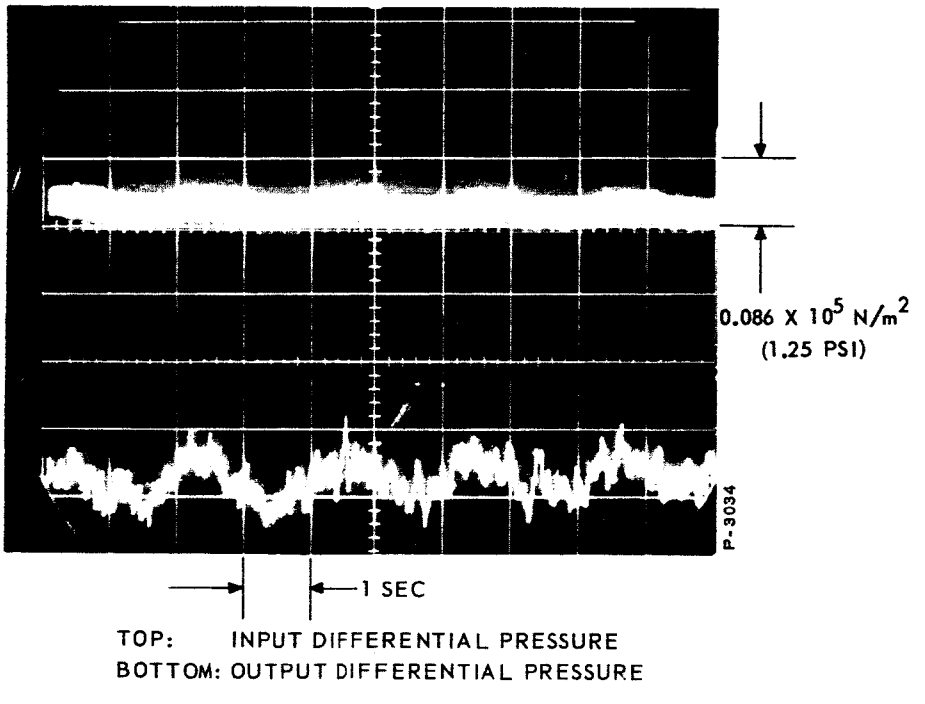

Figure 4-11 - Servovalve Threshold

SECTION 5

CONCLUSIONS AND RECOMMENDATIONS

The results obtained in this program establish the feasibility of implementing practical fluid interaction servovalves. Such servovalves offer important advantages in reliability and maintenance.

The flow recovery of the fluid interaction servovalve is comparable to that of the conventional flapper-nozzle valve. It is also significant to note that the level of the input control pressure is less than the supply pressure and the output pressure differential generated by the servovalve. Hence the servovalve can be controlled by a fluid interaction device having the same (or lower) supply pressure as the servovalve.

It is recommended that additional effort be carried out to achieve improvements in linearity and stability. Better size matching should be achieved between the pilot and power stages to increase flow recovery. Considering the fluid interaction servovalve's inherent capabilities for operating in severe environments, it is further recommended that a model be designed specifically for and tested in severe environments.

APPENDIX A

DESIGN SPECIFICATIONS FOR FLUID INTERACTION PNEUMATIC SERVOVALVE

1. SCOPE

1.1 This specification covers a valve to be designed to meet the requirements of NASA Contract Number NAS3-5212 entitled "Contract for Design, Fabrication and Test of a Fluid Interaction Servovalve."

2. DESCRIPTION OF VALVE

2.1 See block diagram Figure A-1. The input signal is a differential (A minus B) pneumatic signal. The two output ports are arranged so that valve action in one direction opens the supply port S to output port C and opens output port D to return port R. Reverse valve action opens S to D and opens C to R. Since the servovalve operates without moving mechanical parts, the flows through S, R, C, and D cannot be completely shut off. The valve is therefore classified as a pneumatic-input, four-way, open-center, fluid-interaction servovalve.

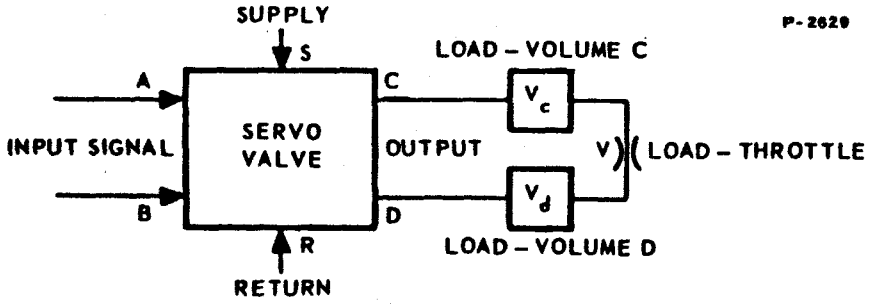

Figure A-1 - Block Diagram of Servovalve and Load

3. SUPPLY PRESSURE & RETURN PRESSURE

P_s = 5.16 x 10^5 N/m^2g (75 psig) dry air at room temperature

P_r = 0 N/m^2g at room temperature

4. SPECIFIED LOAD

4.1 Volumes

$V_c + V_d$ = 164 cm^3 (10 in^3)

V_c min. = V_d min. = 24.6 cm^3 (1.5 in^3)

V_c max. = V_d max. = 139 cm^3 (8.5 in^3)

4.2 Load Throttle

Wide open throttle shall result in a differential pressure across the throttle of less than 0.207 x 10^5 N/m^2 (3 psi) for 0.0113 Kg/sec (0.025 pps) steady flow through the throttle orifice.

4.3 Load Lines

The inside diameter of all lines forming a part of the load shall be greater than 0.76 cm (0.3 inches).

5. SPECIFIED INPUT SIGNAL

5.1 Type

Differential pneumatic signal (signal A minus signal B in Figure A-1) of dry air at room temperature.

5.2 Maximum Pressure

For rated input-signal, each line shall be below 2.75 x 10^5 N/m^2g (40 psig).

5.3 Quiescent Pressure

At zero input-signal, the average of P_a and P_b shall be under 1.38 x 10^5 N/m^2g (30 psig). NASA defines this average as the "pressure bias" of the input signal.

5.4 Maximum Power

The power of an input signal is defined as the product of gage pressure times volumetric flow. The minimum combined power of signals A and B in Figure A-1 shall be less than 30 watts. To get watts, multiply psig times $in^3/sec.$ times 0.113.

5.5 Input Admittance

Variation in admittance of each input due to load throttle changes shall be less than 10 percent of the maximum input admittance, for the complete range of the load throttle from full closed to wide open.

No specification is placed on input admittance as a function of input-signal.

Admittance is defined as the mathematical derivative of input volumetric flow with respect to the absolute pressure in the input line.

6. QUIESCENT SUPPLY FLOW

The flow through line S shall be less than 0.0204 Kg/sec (0.045 pps) at zero input signal. It is desirable that this flow be less than the flow at rated input signal with wide open load throttle.

7. RATED NO-LOAD OUTPUT FLOW

Output flow is defined as flow through the load throttle. The output flow shall be 0.0113 Kg/sec (0.025 pps) for the rated input signal. This is therefore also the definition of rated input signal.

8. FLOW RECOVERY

With wide open load throttle the ratio of output mass flow to supply mass flow shall be greater than 0.55 at rated input signal. Supply mass flow is defined to include only line S in Figure A-1.

9. PRESSURE RECOVERY

The pressure differential across the closed load throttle shall be at least 3.1×10^5 N/m^2 (45 psi) at the rated input signal.

10. QUIESCENT OUTPUT PRESSURE

This is defined as the level of P_c and P_d when $P_c = P_d$. No requirements or preference. NASA defines this as "Output-pressure Bias".

11. DIFFERENTIAL OUTPUT PRESSURE CHANGE PER INPUT POWER CHANGE

With closed load throttle, the change in differential input signal power required to change the differential output pressure from -0.69×10^5 to $+ 0.69 \times 10^5$ N/m^2 (-10 to +10 psi) shall be less than 5 watts.

12. LINEARITY

The ratio of maximum to minimum pressure gain for all values of the input signal shall be less than three (3). "Pressure gain" is defined as the mathematical derivative of the differential output pressure with respect to the differential input signal power during steady operating conditions with closed load throttle.

13. OUTPUT-FLOW VS. DIFFERENTIAL OUTPUT-PRESSURE

The output mass flow shall be equal to or greater than

$$Q_o \left[1 - \frac{P}{P_o} \right]$$

where the quantity Q_o is a constant equal to the output mass flow for a given input signal with wide open load throttle; P_o is a constant and equal to the differential output pressure for the given input signal with closed load throttle; and P is a variable term equal to the differential output pressure for a given input signal and is a function of load throttle setting.

14. OUTPUT STABILITY

Pead-to-peak ripple with closed load throttle shall be less than 0.034×10^5 N/m^2 (0.5 psi) measured after filtering an electrical signal of the differential output pressure with a $1/(0.05S + 1)^2$ filter, for load volumes of V_c minus V_d between -115 and +115 cm^3 (-7 and +7 cubic inches) and for all values of input signal.

15. TRANSIENT RESPONSE

With closed load throttle and equal load volumes ($V_c = V_d = 81.9$ $cm^3 = 5$ in^3), a step input signal for a 0.69×10^5 N/m^2 (10 psi) change in differential output pressure shall result in settling the output within 0.069×10^5 N/m^2 (1 psi) of the final differential output pressure in a time period of less than 0.25 seconds.

16. SYMMETRY

Let γ denote the absolute value of the differential input signal power with closed load throttle. Then the difference in γ for -45 and +45 psi differential output pressures shall be less than 20 percent of the larger of the two values of γ.

17. THRESHOLD

The increment of differential input signal power required to produce a change in output shall be less than 0.5 percent of the difference in the differential input signal power between zero and rated input signal.

18. HYSTERESIS

The difference in the differential input signal power required to produce the same output during a single input cycle shall be less than 3 percent of the difference in the differential input signal power between zero and rated input signal.

19. MATERIAL

Not specified.

20. DIMENSIONS

Not specified.

DISTRIBUTION

NASA-Lewis Research Center (20)
21000 Brookpark Road
Cleveland, Ohio 44135
Attention: Vernon D. Gebben

NASA-Lewis Research Center (2)
21000 Brookpark Road
Cleveland, Ohio 44135
Attention: Lewis Library

NASA-Lewis Research Center (1)
21000 Brookpark Road
Cleveland, Ohio 44135
Attention: James E. Burnett, Technology Utilization Office

NASA-Ames Research Center (1)
Moffett Field, California 94035
Attention: Library

NASA-Goddard Space Flight Center (1)
Greenbelt, Maryland 20771
Attention: Library

NASA-Marshall Space Flight Center (1)
Huntsville, Alabama 35812
Attention: Michael A. Kalange, R-ASTR-NF

NASA-Western Operations (1)
150 Pico Boulevard
Santa Monica, California 90406

NASA Scientific & Technical Information Facility (6 & Reproducible)
Box 5700
Bethesda, Maryland
Attention: NASA Representative

NASA-Lewis Research Center (1)
21000 Brookpark Road
Cleveland, Ohio 44135
Attention: C. J. Shannon

NASA-Lewis Research Center (1)
21000 Brookpark Road
Cleveland, Ohio 44135
Attention: Lewis Technical Information Division

NASA Headquarters (1)
Washington, D. C. 20546
Attention: F. C. Schwenk, NPO

NASA-Flight Research Center (1)
P.O. Box 273
Edwards, California 93523
Attention: Library

NASA-Langley Research Center (1)
Langley Station
Hampton, Virginia 23365
Attention: Library

NASA-Marshall Space Flight Center (1)
Huntsville, Alabama 35812
Attention: Roy E. Currie, Jr. R-ASTR-TN

NASA-Manned Spacecraft Center (1)
Houston, Texas 77001
Attention: Library

Jet Propulsion Laboratory (1)
4800 Oak Grove Drive
Pasadena, California 91103
Attention: Library

Harry Diamond Laboratories (3)
Washington 25, D.C.
Attention: Joseph M. Kirshner

Harry Diamond Laboratories (2)
Washington 25, D.C.
Attention: Library

Wright-Patterson Air Force Base (2)
Ohio
Attention: Library

U.S. Atomic Energy Commission (3)
Technical Information Service Extension
P.O. Box 62
Oak Ridge, Tennessee

NASA-Lewis Research Center (2)
21000 Brookpark Road
Cleveland, Ohio 44135
Attention: Nuclear Rocket Technology Office

NASA Headquarters (1)
Washington, D.C. 20546
Attention: John E. Morrissey, NPO

Army Missile Command (2)
Redstone Arsenal, Alabama
Attention: Library

U.S. Atomic Energy Commission (3)
Technical Reports Library
Washington, D.C.

Los Alamos Scientific Laboratory (1)
Los Alamos, New Mexico
Attention: Joseph Perry, N-4

NASA Lewis Research Center (1)
21000 Brookpark Road
Cleveland, Ohio 44135
Attention: Alan S. Hintze, SNPO

Case Institute of Technology (1)
Mechanical Engineering Department
Cleveland, Ohio
Attention: Prof. Charles Taft

NASA Headquarters (1)
Washington, C.C. 20546
Attention: Herman H. Lowell, REI

NASA-Marshall Space Flight Center (1)
Huntsville, Alabama 35812
Attention: Jerold Peoples,
R-ASTR-NFM

Army Missile Command (1)
Redstone Arsenal, Alabama
Attention: B. J. Clayton

Army Missile Command (1)
Redstone Arsenal, Alabama
Attention: William A. Griffith

Army Transportation & Research Command (1)
(Command (1)
Ft. Eustis, Virginia
Attention: George W. Fosdick

Bolling Air Force Base (1)
Washington, D.C. 20332
Attention: Major C. R. Wheaton

Wright-Patterson Air Force Base (1)
Ohio
Attention: James F. Hall

NASA-Marshall Space Flight Center (1)
Huntsville, Alabama 35812
Attention: William White,
R-ASTR-TN

NASA-Marshall Space Flight Center (1)
Huntsville, Alabama 35812
Attention: Russel Alcott,
R-ASTR-NFM

Army Material Command (1)
Research Division
Washington 25, D.C.
Attention: Major W. T. Kerttula

Army Missile Command (1)
Redstone Arsenal, Alabama
Attention: T. G. Wetheral

Army Munitions Command (1)
Picatinny Arsenal
Dover, New Jersey
Attention: Silvio J. Odierno

Army Transportation & Research
Command (1)
Ft. Eustis, Virginia
Attention: Robert R. Piper

Kirtland Air Force Base (1)
New Mexico
Attention: Capt. Charles V. Fada

Wright-Patterson Air Force Base (1)
Ohio
Attention: Seth A. Young

Wright-Patterson Air Force Base (1)
Ohio
Attention: Ronald Ringo

Office of Naval Research (1)
Department of Navy
Washington, D. C. 20360
Attention: Stanley Doroff

Bureau of Weapons (1)
Munitions Building
Washington 25, D.C.
Attention: Richard A. Retta

Massachusetts Institute of Technology (1)
Department of Mechanical Engineering
Cambridge 39, Massachusetts
Attention: Forbes T. Brown

Wright-Patterson Air Force Base (1)
Ohio
Attention: Charles Bentz

Office of Naval Research (1)
Washington, D.C. 20360
Attention: Ancel E. Cook

U.S. Atomic Energy Commission (1)
Division of Reactor Development
Washington 25, D.C.
Attention: Frank C. Legler

NASA-Lewis Research Center (2)
21000 Brookpark Road
Cleveland, Ohio 44135
Attention: Nuclear Rocket
Technology Office

NASA Headquarters (1)
Washington, D.C. 20546
Attention: Carl Janow, REC

NASA-Langley Research Center (1)
Langley Station
Hampton, Virginia 23365
Attention: H. Douglas Garner

NASA-Flight Research Center (1)
Edwards, California 93523
Attention: Wilton Lock

NASA-Ames Research Center (1)
Moffett Field, California 94035
Attention: E. Perkins

NASA-Manned Spacecraft Center (1)
Houston, Texas 77058
Attention: R. Chilton

NASA-Goddard Space Flight Center (1)
Greenbelt, Maryland 20771
Attention: H. Hoffman

University of Nebraska (1)
Lincoln, Nebraska
Attention: Prof. T. Sarpkaya

NASA-Electronics Research Center (1)
575 Technology Square
Cambridge, Massachusetts 02139
Attention: George Kovatch

NASA-Langley Research Center (1)
Langley Station
Hampton, Virginia 23365
Attention: Harry V. Fuller

NASA-Lewis Research Center (1)
Plum Brook Station
Sandusky, Ohio 44871
Attention: W. E. Kirchmeier

Jet Propulsion Laboratory (1)
4800 Oak Grove Drive
Pasadena, California 91103
Attention: J. Scull

NASA-Lewis Research Center (1)
21000 Brookpark Road
Cleveland, Ohio 44135
Attention: Ruth Weltmann

Aerojet-General Corporation (1)
Liquid Rocket Plant
Sacramento, California
Attention: Mr. Earl Sheridan

University of California (1)
Lawrence Radiation Laboratory
P.O. Box 808
Livermore, California
Attention: Jim Day